

Article

# Symmetry Breaking in Self-Assembled Nanoassemblies

Yutao Sang <sup>1,2</sup>  and Minghua Liu <sup>1,2,3,\*</sup>

<sup>1</sup> CAS Key Laboratory of Colloid, Interface and Chemical Thermodynamics, Institute of Chemistry, Chinese Academy of Sciences, Zhongguancun North First Street 2, Beijing 100190, China

<sup>2</sup> University of Chinese Academy of Sciences, Beijing 100049, China

<sup>3</sup> Collaborative Innovation Centre of Chemical Science and Engineering, Tianjin 300072, China

\* Correspondence: liumh@iccas.ac.cn

Received: 26 June 2019; Accepted: 18 July 2019; Published: 25 July 2019



**Abstract:** The origin of biological homochirality, e.g., life selects the *L*-amino acids and *D*-sugar as molecular component, still remains a big mystery. It is suggested that mirror symmetry breaking plays an important role. Recent researches show that symmetry breaking can also occur at a supramolecular level, where the non-covalent bond was crucial. In these systems, equal or unequal amount of the enantiomeric nanoassemblies could be formed from achiral molecules. In this paper, we presented a brief overview regarding the symmetry breaking from dispersed system to gels, solids, and at interfaces. Then we discuss the rational manipulation of supramolecular chirality on how to induce and control the homochirality in the self-assembly system. Those physical control methods, such as Viedma ripening, hydrodynamic macro- and micro-vortex, superchiral light, and the combination of these technologies, are specifically discussed. It is hoped that the symmetry breaking at a supramolecular level could provide useful insights into the understanding of natural homochirality and further designing as well as controlling of functional chiral materials.

**Keywords:** symmetry breaking; assemblies; supramolecular chirality; homochirality; self-assembly; vortex

## 1. Introduction

Chirality is one of the fundamental properties found in nature and also vital in many fields, including chemistry, physics, biochemistry, pharmacy, and materials science [1–5]. The chirality of molecular components has dramatic consequences in life systems, where biological homochirality, e.g., *L*-amino acids and *D*-sugar are solely selected, still remains a big mystery [6,7]. It has a profound effect across a spectrum of disciplines in both industrial and academic researches [8,9]. Beyond the molecule level, the chirality is extended down to subatomic and up to supramolecular and higher hierarchical levels [10]. The biological DNA double helixes and helical proteins are the typical consequence of molecular chirality and formed via self-assembly at a supramolecular level. In these chiral nanostructures, the structural complexity, information storage, and the realization of complicated functions significantly related to the chirality. At a supramolecular level, many chiral or achiral molecules prefer to self-assemble into an asymmetric packing mode, thus we could detect supramolecular chirality from various combinations of chiral and achiral molecules [11,12]. Generally, the chirality can be expressed from the chiral molecules to the self-assembled assemblies via non-covalent bonds. For the mixed system including chiral and achiral building blocks, the chirality can be transferred from the chiral components to achiral components, and thus endowing the achiral molecules with supramolecular chirality. Apart from that, even exclusively achiral molecules can form chiral aggregates due to the symmetry breaking [13–17]. While in most of the cases, an equal amount of the right and left-handed assemblies appeared from achiral molecules, predominant chiral aggregates have also been found. However, while these systems are interesting, a great challenge remains in controlling the supramolecular chirality or achieving the homochiral assemblies from the stochastic distributions.

It is generally believed that homochirality is attained in consecutive steps: starting from a minute chiral bias, and a subsequent chiral amplification process for enantiomeric enrichment and chiral transmission from one set of molecules to another [18,19]. For the first stage, the chiral bias is usually generated by the symmetry breaking. For the second stage, amplifying chirality by using self-assembly is a well-known strategy in supramolecular assemblies [11]. Therefore, exploring the symmetry breaking in self-assembled nanoassemblies is crucial and inspired for the understanding of biomolecular homochirality during the evolution of life [19–23].

In this review, we will firstly present a brief synopsis of symmetry breaking in self-assembled systems, including crystals, liquid crystals, air/solution and solution/solid interface, and supramolecular gels. After that, we pay more attention to the manipulation of supramolecular chirality in the self-assembled systems by physical or chemical ways such as adding chiral dopants, applying Viedma ripening, hydrodynamic macro- and micro-vortex, superchiral light, and the combination of these technologies. Those physical control ways are mostly discussed.

## 2. Symmetry Breaking in Self-Assembly Systems

Over the past two decades, spontaneous symmetry breaking has been found in various self-assembly systems including crystals [24–26], Langmuir monolayers [27–29], liquid/solid interface [30–32], liquid crystals [33–37], dye aggregates [14,16,38,39], amphiphilic assemblies [40,41], and supramolecular gels [42–47]. Figure 1 illustrates some typical examples in these field. One chiral crystal that has been investigated in detail is tartrate [48]. During crystallization process, two kinds of chiral crystals with almost identical physical properties can be formed. However, the plane of polarization rotates are different when linearly polarized light (LPL) passes through these chiral crystals. It should be noticed that their optical activity maintains when these crystals are dissolved in water. However, another well-studied crystal with chirality in solid, named as sodium chlorate ( $\text{NaClO}_3$ ), behaves quite differently, as it displays optical activity in crystal state (Figure 1A), but the optical properties disappears when the crystal totally dissolves in solution [49,50]. It is known that a crystal exists in a molecular or ion state in solution. Therefore, the above phenomenon suggests that ions of tartrate molecules are chiral. Conversely, the ions of the  $\text{NaClO}_3$  molecule are achiral. This is one typical example of symmetry breaking in crystal systems, and thereafter many achiral molecules have been found to be chiral in crystals [51–55].

Apart from a few reports of symmetry breaking in solution [16,38,56–59], the introduction of an interface is effective to control the intermolecular interactions, thereby affecting their self-assembly properties. The symmetry also can be broken at a confined two-dimensional (2D) surface/interface during the self-assembly of achiral building blocks [60]. In fact, the formation of symmetry breaking at a surface/interface is more common than chiral crystallization in three dimensions [61]. However, compared with the solution state, the analysis of assemblies at surfaces/interface can be more complicated. For example, the chiral domains are usually hard to distinguish and the artefacts can confound the optical spectroscopy measurements. Even so, the study of symmetry breaking on surfaces and at interfaces not only assists our understanding of three-dimensional crystallization and self-assembly process, but also provides insight into how to fabricate otherwise complicated chiral materials, such as chiral graphene nanoribbons [62,63].

Among many kinds of 2D materials, Langmuir–Blodgett (LB) technology is an effective method to orderly arrange molecules on the interface [64,65]. Figure 1B gives a novel type of chiral assemblies fabricated from achiral amphiphilic molecules, a derivative of barbituric acid [28]. This molecule could form a chiral LB films at the air/water interface. As shown in the atomic force microscope (AFM) images, this LB film was consisted of spiral nanoarchitectures. More interestingly, these spirals were found to wind in both an anticlockwise (CCW) and a clockwise (CW) direction, and a careful investigation indicated this morphology was closely depended on the surface pressure. It was noted that the H-bonding between barbituric acid derivatives themselves is crucial for the self-assembly. Specifically, the carbonyls in 4- and 6-carbonyl of the pyrimidinetrione could form H-bonds with the



interdigitation interactions between neighbouring molecules at the liquid–solid interface were found to be crucial for the fabrication of the porous network structures [66].

In liquid crystal systems, there are many pioneering works that leading the research of symmetry breaking [33,35,70,71]. This is because liquid crystal is one unique phase that lies in between the crystals (or solid) and diluted solution. Different from the crystals, the weak intermolecular interactions in liquid crystal indicates that the driving force for chirality (long-range helical order) is relative weaker. On the other hand, the short-range chirality in liquid crystals is retained compared with the solution state. This combination leads to many distinct features, such as stimuli-responsive, self-healing, and adaptive behavior, which makes liquid crystals as the quintessential materials for self-assembly and symmetry breaking [72–74]. As shown in Figure 1D, when the crossed analyser and polarizer were slightly rotated, two kinds of domains are observed in some of the cubic phases [34]. Remarkably, when the rotation of the analyzer is reversed, the darker and brighter domains could exchange their contrast. However, the contrast does not change when the sample is rotated between the fixed polarizers, indicating that these domains belongs to a chiral structure with opposite handedness [34].

Recently, many achiral molecules, particularly the  $C_3$ -symmetric structure molecules, are found to form helical assemblies in supramolecular gel systems [45,75]. For example, as shown in Figure 1E, chiral symmetry breaking phenomena are observed in the supramolecular gel of achiral benzene-1,3,5-tricarboxamide/tricarboxylate-based molecules [43,46,67]. The directional H-bonds between amide groups and the  $\pi$ – $\pi$  stacking of the benzene rings are the main driven force during self-assembly process. When three non-chiral ethyl cinnamates were connected to the central benzene-1,3,5-tricarboxamide, the molecule was found to form instant gels with unequal number of right (*P*) and left (*M*)-handed twists, as observed from the scanning electron microscope (SEM) images in Figure 1E [43]. If the sample has more *M*-type twists than *P*-type twists, a negative Cotton effect was observed from the circular dichroism spectra; this was reversed if there were a relatively larger amount of *P*-type twists. Therefore, the uneven symmetry leads to the bulk macroscopic chirality of the supramolecular gels.

Based on the experimental data and the molecular dynamics simulation, it shows that the aggregation of these achiral  $C_3$  molecules could initially form predominantly *P*-type or *M*-type aggregates with a random distribution. Thereafter, due to the steric hindrance caused by the closing-molecular packing, the subsequently growth of those small helical aggregates will follow the original chirality to form one-dimensional helical aggregates. Finally, such unequal numbers of *P*-type and *M*-type helical aggregates further twisted into twisted ribbons or larger helical fibers and intertwined with each other to hold the solvent [43].

It should be noted that appropriate manipulation of different noncovalent interactions can fabricate chiral ordered structures with various dimensions and complexities, which might be comparable with that found in nature systems. Among these noncovalent interactions, the hydrogen bond (H-bond) is crucial due to its directionality, strength, specificity of the interaction, and biological relevance [76–80]. For example, as shown in Figure 2A, 2,4-Diamino-6-phenyl-1,3,5-triazines with a single oligo (ethylene oxide) chain could form an optically isotropic mesophase [81]. This achiral molecule first formed a primarily double-hydrogen-bonded dimeric aggregates, and these aggregates paralleled side-by-side, leading to a highly ordered and hydrogen-bonded aromatic bilayer structures. Interestingly, the ethylene oxide chain at both ends prohibits the parallel alignment of the hydrogen-bonded cores, and thus induces a small helical twist between them. After that, the helical deformation of the bilayer ribbons is formed. The results shown that hydrogen bonding leads to chiral aggregates that undergo long-range chirality synchronization in the isotropic bulk state [81].

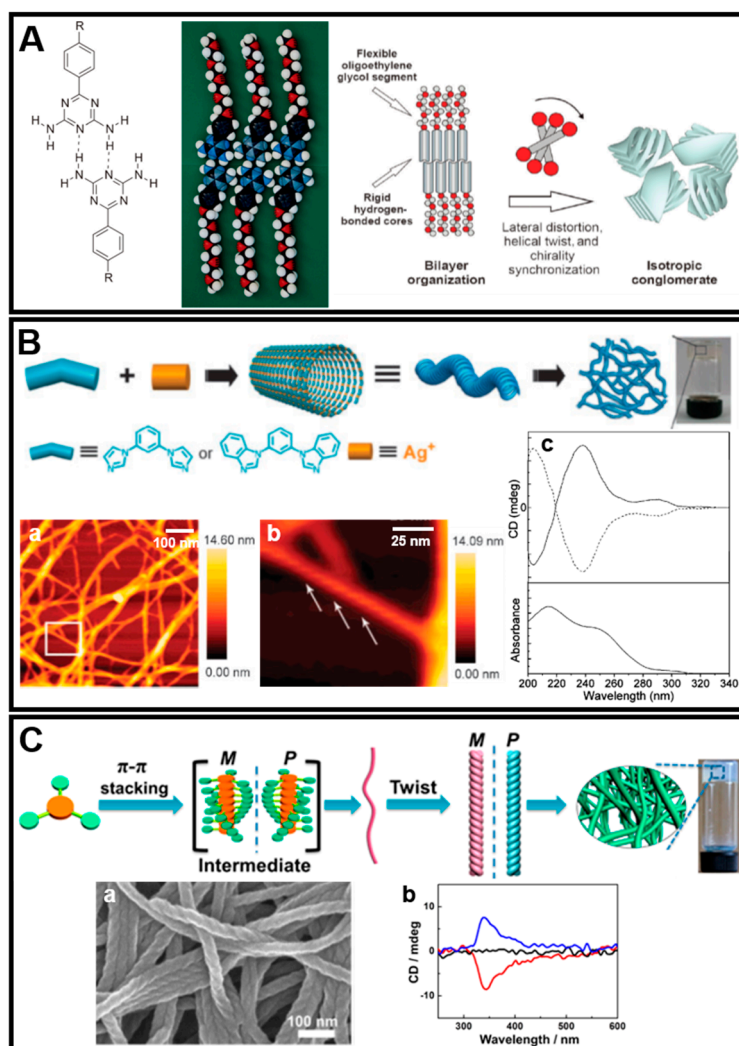


**Figure 2.** (A) Double hydrogen bonding, Corey-Pauling-Koltun (CPK) model and the scheme illustration of the chirality synchronization of hydrogen-bonded complexes of achiral N-heterocycles. Reprinted with permission from ref. [81]. (B) Schematic representation of the self-assembly process of the coordination polymers. (a) Tapping-mode atomic force microscope (AFM) height image and (b) a zoomed-in image of the area marked in (a). (c) Corresponding CD and UV-Vis spectra. Reprinted with permission from ref. [17]. (C) The possible gelation process (a) SEM image and (b) CD spectra of the chiral gels. Reprinted with permission from ref. [44].

Besides the hydrogen bond, there are a number of examples of dative-bond (coordination bond) driven symmetry breaking [82–86]. Figure 2B shows a novel coordination polymer gelators that stemmed from the coordination of  $\text{Ag(I)}$  and the achiral imidazole derivative [17]. Optically transparent gels could be formed when a methanol solution of the achiral monomer to an aqueous solution of silver nitrate at a 1:1 ratio of ligand:  $\text{AgNO}_3$ . The AFM measurements further revealed a well-developed network structure composed of fibrous aggregates. In addition, the zoomed-in image indicated that this thicker fiber consisted of a bundle of helical tubes. The CD spectra also exhibited mirror-imaged signals from different batches, indicating that chiral symmetry breaking is occurred during the coordination process. Due to the strong directional interactions between the rigid bent bridging ligands and  $\text{Ag(I)}$ , the initial metal–ligand complexes with accidental excess of one helical direction were formed. Thereafter, the new aggregates would follow the same handedness to form a secondary helical structure. On the other hand, the formation of opposite helical aggregates is suppressed. Therefore, the eventual macroscopic chirality is observed [17].

As shown in Figure 2C, symmetry breaking that driven exclusively by weak  $\pi$ - $\pi$  interaction is studied in supramolecular assemblies [44]. An achiral  $C_3$ -symmetric gelator was found to form organogels in cyclohexane. Interestingly, the supramolecular gels were optically active with the helical nanofibers with predominant handedness. Since there are no any other noncovalent interactions in this system, the experiment results proved that purely  $\pi$ - $\pi$  stacking can also drive the symmetry breaking in the supramolecular gel system. In this case,  $\pi$ - $\pi$  interaction between benzene rings and cinnamate substituents were strong enough to form an overcrowded molecular packing. It is supposed that the achiral molecules could initially generate two kinds of helical conformer by chance, and subsequently grow up to form longer one-dimensional helical aggregates by following the original chiral conformation. At last, several helical aggregates further twisted into helical fibers [44].

In fact, combined noncovalent interactions including hydrogen bonding, electrostatic interaction, and  $\pi$ - $\pi$  stacking are generally necessary in most of the symmetry breaking systems. For example, both the hydrogen bonding and electrostatic interaction is essential in the fabrication of chiral tetraphenylporphyrin sulfonate (TPPS) aggregates [14]. Another example is the self-assembled achiral partially fluorinated benzene-1,3,5-tricarboxamides in solution, in which the 3-fold hydrogen bonding and dipole-dipole interaction play important roles [42].

### 3. Selection and Control of Supramolecular Chirality during Symmetry Breaking: Towards the Homochirality in Nanoassemblies

Even though the origin of chirality and homochirality in biological systems is still controversial, the quest to unravel this mystery has led to an intense research to select and control the supramolecular chirality during symmetry breaking. Actually, the manipulation of chirality in exclusive achiral systems can be much more useful, since it could not only provide a better understanding of the complicated biosystems, but also offer guidance on how to rational design of biomimetics as well as advanced chiral materials [87,88]. To date, various strategies such as changing pH [89], electrostatic interaction [90,91] and microfluidic conditions [92,93], catalysis at prochiral crystal surfaces [94,95], adding chiral additive [96–99], applying circularly polarized light [100–102], rotational and magnetic force [103], and vortex and stirring motion [14,104–108], etc. are known to control the emerging chirality during symmetry breaking.

Generally, based on sergeant and soldier rule, adding chiral substance into the symmetry breaking systems is quite efficient and usual to control the macroscopic chirality [99,109,110]. For example, in the  $C_3$  supramolecular gel system, a suitable amount of (*R*)-1-cyclohexyl ethylamine could result in the formation of *M*-type twists with a strong negative CD signal [43]. On the contrary, (*S*)-1-cyclohexyl ethylamine led to the *P*-type twists and a mirror-imaged CD spectrum. Owing to the interaction between amines and ethyl cinnamate, the added chiral amines achieved the chirality control through the ester–amide exchange reaction. In this case, the chiral amines could not completely remove from the system [43]. However, if the chiral dopants were replaced to chiral solvent, such as limonene and terpinen-4-ol, the induced chirality of the supramolecular gels could be maintained even after completely removing the chiral solvents [44].

In the solid state such as crystal systems, it is easier to achieve the chiral discrimination. Particularly, this applies to the crystallization process when the same enantiomers have a stronger interaction than that of the opposite enantiomer. Such kind of crystal is generally called as conglomerate crystals, representing that each crystal is homochiral (Figure 3A). In the words, the conglomerate can be regarded as a physical mixture of enantiomerically pure crystals of two kinds of enantiomer. However, only approximately 5–10% of chiral crystalline molecules belong to this case [9]. For the rest of approximately 90–95%, both enantiomers exist in one crystallographic unit cell, and the solid is called a racemic compound, racemate crystals, or true racemate. This is because the opposite enantiomers have a greater affinity than the same enantiomer in this case.

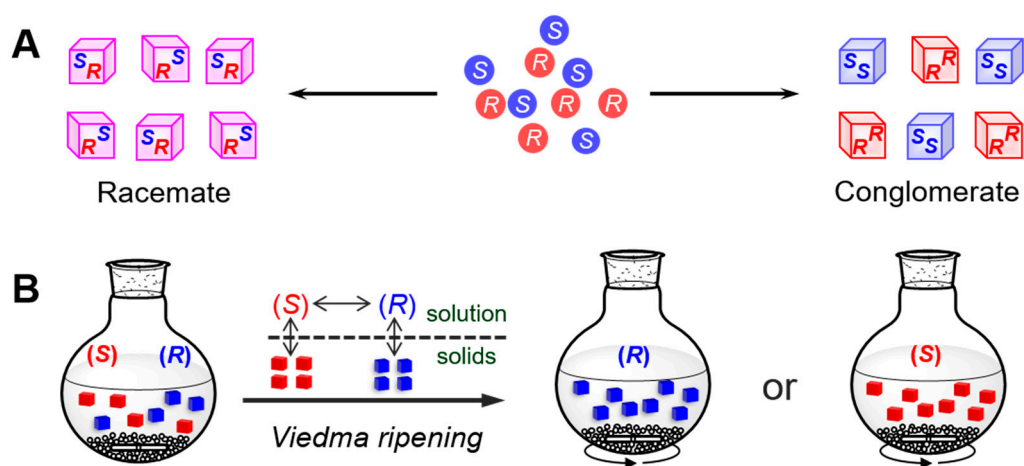


**Figure 3.** (A) Formation of conglomerate and racemate crystals during the crystallization of a racemic mixture. (B) Schematic representation of Viedma ripening.

It is worth noting that applying stirring during crystallization is usually effective to break the symmetry, leading to a high enantiomeric excess of the resulting crystal [25,111,112]. In 2005, Viedma demonstrated that the initially racemic mixture of  $\text{NaClO}_3$  crystals could completely transform into one chiral form over a period of several days (Figure 3B) [113]. Remarkably, the completely transformation means that the whole system achieves homochirality although the final handedness could not control. This transformation process, which is now called Viedma ripening, involves the deracemization of solid-to-solid and solution-to-solid [114,115]. The novelty of Viedma's experiment lies in the addition of glass beads and magnetic bar during deracemization. The glass beads enhanced the grind of crystals, resulting in numerous small fragments with the identified handedness. Therefore, the homochirality is achieved by applying stir and grind for a period of time. It should be noted that the chiral bias can be controlled by crystal enantiomeric excess [113]. For example, solutions with initial 5% *L*-crystal enantiomeric excess give rise to 100% *L*-type crystals, and vice versa. Since that, this method was successfully extended to many crystal systems, and even organic reaction which contains crystal products. Very recently, Viedma ripening found broad applicability [18,116–122]. Without grinding treatment, a temperature gradient which involves several cycles of rapid heating and slow cooling could also realize the deracemization [123,124].

The responses of achiral molecules and its chiral assemblies to external stimulation can be also used to manipulate the supramolecular chirality after symmetry breaking. The J-aggregates of achiral amphiphilic porphyrins, such as 4-sulfonatophenyl and arylmeso-substituted porphyrins, may be the most representative model for the study of hydrodynamic forces [106,125]. Figure 4 illustrates the ground-breaking work of Ribo et al. in which the chiral signal of porphyrin aggregates can be controlled by vortex motion during self-assembly process [14]. The self-assembly of the achiral monomeric species were promoted by the rotary evaporation of very diluted solutions of deprotonated porphyrins.

Clearly, the randomly distributed chiral signals indicates that the unstirred experiments belong to a pure symmetry breaking process (Figure 4A). However, as shown in Figure 4B, the chiral selection was dependent on the rotation direction when the samples were applied rotary evaporation treatment. The statistical distribution indicated that 85% of the chiral signals could be controlled by the rotation direction, suggesting a biased symmetry breaking (Figure 4B). Due to the existence of anionic sulfonato groups and the positively charged porphyrin rings, the J-aggregation was achieved by the intermolecular electrostatic and hydrogen bonding interactions. Therefore, the arrangements of achiral porphyrins with different angles are indeed possible (Figure 4C). The schematic illustration shows that the chirality may be transferred from the macroscopic chiral force to the electronic distribution. After this report, the acting chiral hydrodynamic shear force during rotatory evaporation were theoretically investigated, and similar conclusions has been obtained in other type of vortices [126–129].

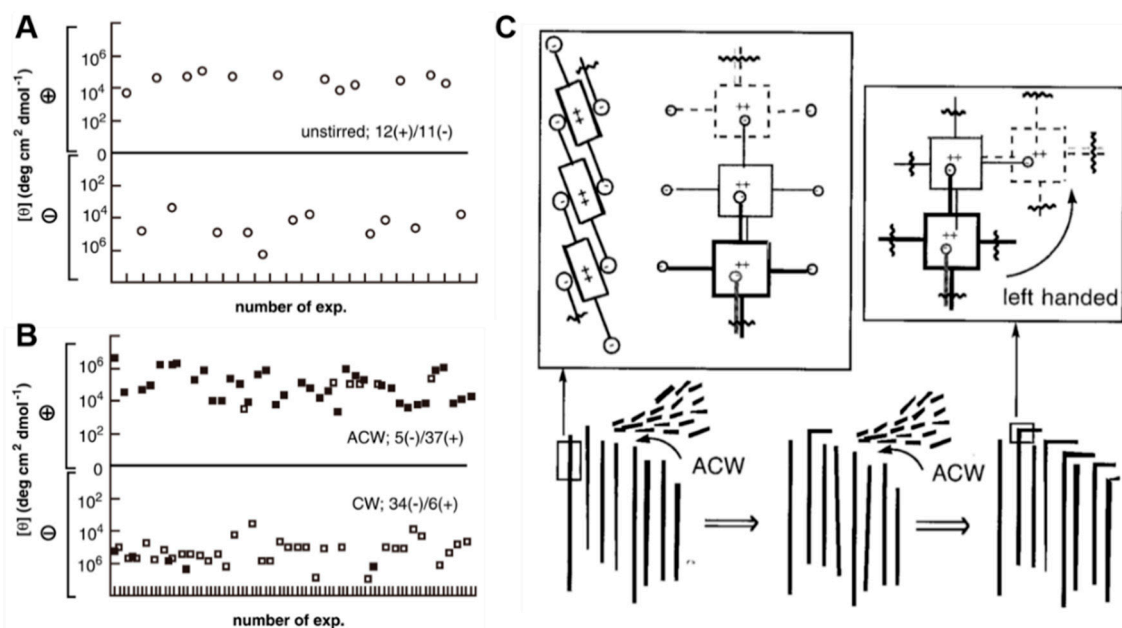


**Figure 4.** The chiral signals of solutions containing achiral amphiphilic porphyrins under (A) unstirred condition and (B) rotatory evaporation. The concentration was conducted by rotatory evaporation from 500 mL to 20 mL for about 2 h. (C) Schematic illustration of the chiral selection during the self-assembly of substituted porphyrins. Reprinted with permission from ref. [14].

As one kind of the excited-state optical activity, circularly polarized light (CPL) has triggered intense research interests due to their potential applications in optical sensors [130,131], 3D displays [132,133], bioencoding [130,134,135], encrypted transmission, and storage of information [136], chiral catalysts [137–140], and photoelectric devices [141]. However, due to the small anisotropy factors ( $<10^{-3}$ ), the obtained enantiomeric excess in most cases of asymmetric photolysis and photosynthesis is undesirable ( $<4\%$ ) [142,143]. When two counter-propagating CPL are interfered with opposite handedness, with different intensity but the same frequency, the generated light, which is called superchiral light (SCL), was demonstrated experimentally to enhance the enantioselective polymerization of achiral diacetylene monomer [144].

Figure 5A shows the experimental set-up for the generation of SCL from two CPL beams (325 nm) [144]. Clearly, compared with the conventional CPL, the achiral benzaldehyde-functionalized diacetylene (Figure 5B) LB films that irradiated by the SCL exhibited a stronger CD signal. In contrast, if the sample was polymerized by LPL, no signal was observed from the CD measurement (Figure 5C). As a result of the enhanced optical dissymmetry, the polydiacetylene films achieved in SCL field shows nearly 5-fold enhancement in dissymmetry factor. As illustrated in Figure 5D,E, compared with CPL irradiation, the enhanced optical dissymmetry in SCL may lead to more helical polydiacetylene (PDA) chains, thus resulting in an increased dissymmetry factor of PDA films. In addition, transmission electron microscopy (TEM) images also demonstrated that samples polymerized by SCL have more helical PDA chains than those polymerized with CPL [144].

Although all of the above approaches can be used alone to select the supramolecular chirality, not all of them are effective, due to their own limitations. In fact, a large number of reports employed more than one treatment to control the chirality of symmetry breaking [145]. For example, as shown in Figure 6A, Vlieg et al. demonstrated that the CPL irradiation caused symmetry breaking of an amino acid derivative could be amplified by a grinding process [146]. Specifically, a solid–liquid mixture was firstly irradiated with *L*- or *R*-CPL for 70 h (0.3 mW intensity). Thereafter, the slurry was grinded with a magnetic stirring bar and glass beads. In addition, organic base such as 1,8-diazabicyclo [5.4.0] undec-7-ene (DBU) was added in order to induce the racemization in solution. Five days later, the final chirality of enantiopure solid was found to be selected by the handedness of CPL. From the above

description, it can be concluded that a non-racemizable chiral photoproduct may be formed under the effect of the CPL irradiation, while the subsequent grind treatment amplified the small initial chirality [146].

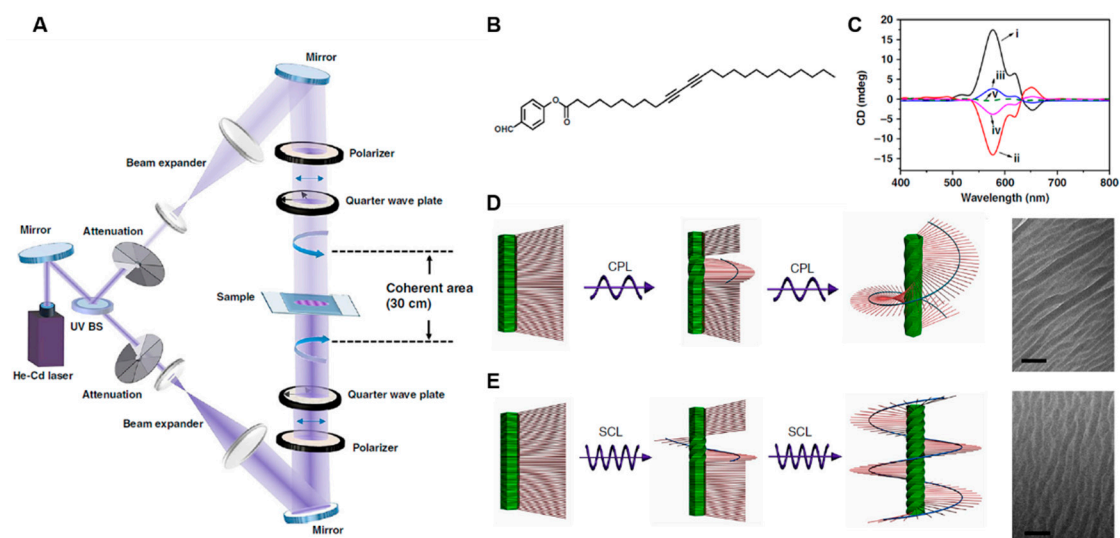


**Figure 5.** (A) Experimental set-up for the generation of superchiral light (SCL) field. (B) The molecular structure of achiral benzaldehyde-functionalized diacetylene. (C) CD spectra of polydiacetylene films polymerized by (i) left-handed or (ii) right-handed SCL; (iii) left-handed or (iv) right-handed circularly polarized light (CPL); (v) linearly polarized light (LPL), respectively. Schemes and corresponding transmission electron microscope (TEM) images for the helical PDA chains prepared by using (D) CPL and (E) SCL irradiation, respectively. Reprinted with permission from ref. [144].

Figure 6B gives an example of how the relative directions of rotation and effective gravity control the chirality of supramolecular assemblies constructed by achiral tris-(4-sulfonatophenyl) phenylporphyrin (TPPS<sub>3</sub>) [103]. In order to simultaneously realize the manipulation of rotational, gravitational and orienting forces, an experiment set-up is designed and outlined in Figure 6B. To be brief, this set-up contains a tube with seven cylindrical vessels. Each of them was positioned at different positions and rotated for various time. Such a set-up ensures a solid-body rotation, and thus avoids the creation of pseudovortices. The rotation is characterized by two parameters, one is the angular momentum ( $L$ ), which is set by CW or CCW rotation viewing from the top. The other factor is effective gravity ( $G_{\text{eff}}$ ) that related to the magnetic levitation force. After rotation treatment, these samples were placed outside the magnet for three days before the CD measurement. The handedness of the aggregates is found to depended on the relative directions of the rotational and gravitational forces applied. For example, the antiparallel  $L$  and  $G_{\text{eff}}$  results in a positive CD signal, while parallel  $L$  and  $G_{\text{eff}}$  leads to the opposite signals. Further study revealed that the nucleation step was crucial to control the final handedness. On the basis of these experimental results, a possible schematic model was proposed. As a result of the electrostatic and  $\pi$ -stacking interactions, the TPPS<sub>3</sub> molecules could aggregate into small chiral nucleus. During this period, the hydrodynamic flow consistently applied. Meanwhile, the magnetic field arranges the nuclei along the rotation axis, which eliminated the randomizing Brownian motion and thus achieved the controlled chirality. After that, chiral nuclei worked as chiral seeds, and the subsequent growth followed the initial chirality even after the external stimulation was ceased [103].

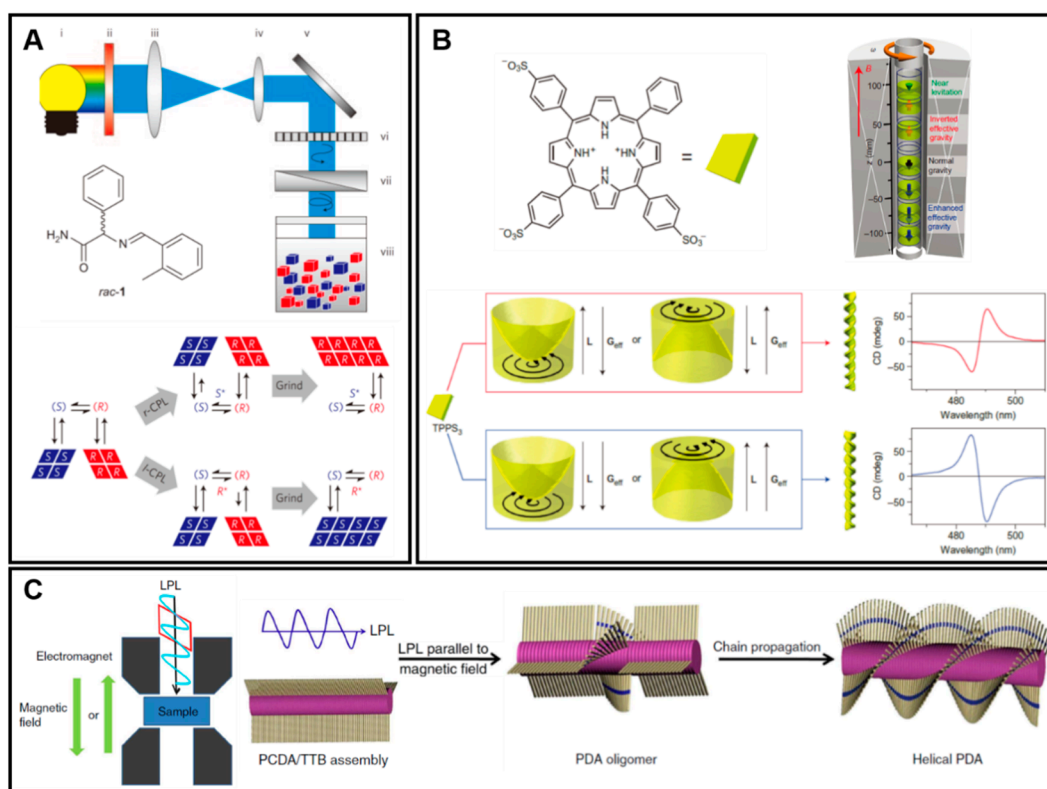


**Figure 6.** (A) Experimental set-up for circularly polarized light (CPL)-driven deracemization and the illustration of the cascade of events during this process. Reprinted with permission from ref. [146]. (B) Molecular formula of the achiral porphyrin tetraphenylporphyrin sulfonate (TPPS<sub>3</sub>), experimental set-up and the relationship between the chirality and the applied physical forces. Reprinted with permission from ref. [103]. (C) Experimental set-up and the possible helix formation mechanism for the enantioselective synthesis of helical polydiacetylene by applying linearly polarized light (LPL) and magnetic field. Reprinted with permission from ref. [137].

Compared with CPL, the application of LPL irradiation is usually neglected. However, combined with other physical force, such as magnetic field, LPL is also effective to control the enantioselective polymerization of diacetylene derivative (Figure 6C) [137]. As a result of the magnetochiral dichroism effect, the achiral building blocks could selectively form one-handed helical oligomer chain. The dual effect of LPL and magnetic field might orient the helical oligomer chain in a chiral arrangement, which is benefit for the polymerization of closing monomer. Therefore, the final predominant helical chains can be directed by the relative orientation of LPL and magnetic field [137].

Very recently, inspired by natural rock micropores (Figure 7A), a microvortex generated by a microfluidic device was demonstrated to control the chirality after symmetry breaking either in gel or solution states [93]. Computational fluid dynamics (CFD) simulation suggested that the CCW and CW laminar vortices could be generated by the mismatched flow velocities between the main channel and the microchambers, and the microvortices in the left and right microchamber are predominantly *P* and *M* chirality, respectively. In addition, the high-speed microscopic observation showed that the highest rotation speed could be  $4 \times 10^4$  rpm in this device. When the achiral building blocks (BTAC and TPPS<sub>4</sub>) were injected into the microfluidic device, microvortex-induced symmetry breaking of these achiral molecules leads to the formation of supramolecular gels or TPPS<sub>4</sub> nuclei. Samples that obtained from two outlets always exhibited mirror-imaged CD signals. The unique feature of microvortices is the strong shear gradient, which allows the chiral alignment and formation of the supramolecular nuclei against the Brownian regime during the mirror symmetry breaking process. The microvortice controlled nuclei could be subsequently amplified into supramolecular aggregates with a certain

chiral bias. As a result, the chirality distribution suggested the microvortices maintained 96% chirality control [93].

Compared with crystals, the homochirality after symmetry breaking is more difficult to achieve in soft matter and solution due to the dynamic features. In addition, the good stability of chiral assemblies is also essential. For example, the exchange between the monomers and helical aggregates is usually fast in diluted solution [99]. Figure 7B illustrated a novel strategy for obtaining almost homochiral supramolecular assemblies with controlled handedness in a totally achiral system [67]. Due to the hydrogen bond and  $\pi$ - $\pi$  stacking, the achiral  $C_3$  molecules could form instant gels in a mixed solvent of DMF/H<sub>2</sub>O. However, the common gelation process only achieved racemic gels. Interestingly, applying vortex mixing during self-assembly process could significantly amplified the supramolecular chirality, leading to near-unity homochiral assemblies. In this case, the chiral signals were random distributed. The real-time monitor of CD intensity and the aggregation suggested that applying vortex mixing during the nucleation stage is sufficient. Due to the competition caused by vortex mixing, one kinds of helical nuclei occasionally dominated the system, and the chiral bias could be further amplified in the following growth. More importantly, by using a small amount of assemblies obtained as chiral seeds, a supramolecular ripening process could transform the racemic gels to the homochiral state with the seeds. Therefore, no additional chiral substances are required to obtain both chirality controlled and homochiral assemblies [67].

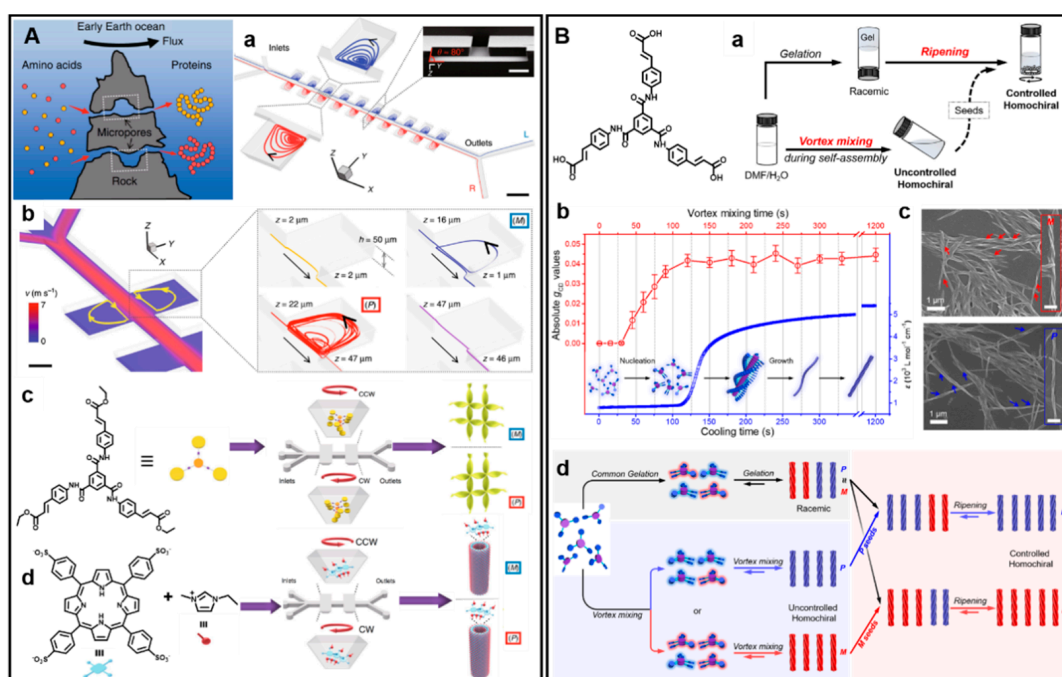


**Figure 7.** (A) Schematic hypothesis of the origin of supramolecular chirality in nature. (a) The imitated microvortices that generated by the microfluidic device. (b) computational fluid dynamics (CFD) simulation of the chiral microvortices. Formation of chiral supramolecular assemblies of achiral (c) (tris (ethyl cinnamate) benzene-1,3,5-tricarboxamide (BTAC) and (d) tetraphenylporphyrin (TPPS4) and C<sub>2</sub>mim<sup>+</sup> ionic stabilizer within the microvortices. Reprinted with permission from ref. [93]. (B) Vortex mixing-accompanied self-assembly induced homochiral supramolecular assemblies from exclusively achiral molecules. (a) Schematic illustration of the procedures towards homochirality. (b) Red curve: the absolute dissymmetry factors ( $g_{CD}$ ) of the samples prepared with different vortex times; blue curve: the correlation between the absorption data and cooling time. (c) SEM images of the helical structures after vortex mixing. (d) Schematic illustration of the mechanism towards homochirality. Reprinted with permission from ref. [67].

#### 4. Conclusions

Symmetry breaking in self-assembled systems is an interesting phenomenon leading to an understanding of the homochirality in a biological system and providing an important method towards the construction of functional chiral materials, which significantly extend the potential applications of achiral building blocks. This review provides a summary and discussion of symmetry breaking based on the diverse systems from solution, interfaces to solids and gels. Moreover, we present a brief synopsis on the selection and control of supramolecular chirality in the self-assembled systems from achiral molecules. A number of novel physical manipulations, such as superchiral light field, microfluidic device induced microvortex, and vortex mixing have been successfully used to achieve the chiral selection/synthesis and even homochirality of nanoassemblies.

Despite these achieved developments in symmetry breaking, advanced techniques are still needed to follow the symmetry breaking process and the amplification of the supramolecular chirality from completely achiral molecules. For most of the systems, even though we could observe the microscopic chirality from the CD or CPL spectra and morphology, two enantiomers coexisted after symmetry breaking. Therefore, it is also necessary to quantitatively analyze the enantiomeric excess of the supramolecular assemblies although it is dynamic in many cases.

So far, various possibilities have been proposed to explain the emergency of the initial chiral bias in biomolecules [101,147–149]. However, these results are controversial [19,150]. On the other hand, attaining homochirality is still a challenge in exclusively achiral systems. In general, asymmetric environments or elements are necessary for the chirality control of symmetry breaking. Macroscopic chiral force caused by stirring or vortex mixing may transfer the chirality into the asymmetry molecule aggregation. Although many methods were discovered to control the chirality, the combination of two or more processes is more effective to the selection and subsequent amplification the supramolecular chirality during symmetry breaking towards the homochiral assemblies, which may enlighten the understanding the of biomolecular homochirality during the evolution of life.

**Author Contributions:** Both authors contributed to the writing and editing of this review.

**Funding:** This research was funded by Strategic Priority Research Program of the Chinese Academy of Sciences (XDB12020200), Key Research Program of Frontier Sciences, CAS (QYZDJ-SSWSLH044), and National Natural Science Foundation of China (21890734).

**Acknowledgments:** The authors gratefully acknowledge their collaborators whose names appear in the literature cited and the insightful comments from three reviewers.

**Conflicts of Interest:** The authors declare no conflict of interest.

#### References

1. Chelucci, G.; Thummel, R.P. Chiral 2,2'-bipyridines, 1,10-phenanthrolines, and 2,2': 6',2''-terpyridines: Syntheses and applications in asymmetric homogeneous catalysis. *Chem. Rev.* **2002**, *102*, 3129–3170. [[CrossRef](#)] [[PubMed](#)]
2. Chin, J.; Lee, S.S.; Lee, K.J.; Park, S.; Kim, D.H. A metal complex that binds alpha-amino acids with high and predictable stereospecificity. *Nature* **1999**, *401*, 254–257. [[CrossRef](#)] [[PubMed](#)]
3. Engelkamp, H.; Middelbeek, S.; Nolte, R.J.M. Self-assembly of disk-shaped molecules to coiled-coil aggregates with tunable helicity. *Science* **1999**, *284*, 785–788. [[CrossRef](#)] [[PubMed](#)]
4. Lehn, J.M. Supramolecular chemistry. *Science* **1993**, *260*, 1762–1763. [[CrossRef](#)] [[PubMed](#)]
5. Prins, L.J.; Huskens, J.; de Jong, F.; Timmerman, P.; Reinhoudt, D.N. Complete asymmetric induction of supramolecular chirality in a hydrogen-bonded assembly. *Nature* **1999**, *398*, 498–502. [[CrossRef](#)]
6. Bada, J.L. Biomolecules - origins of homochirality. *Nature* **1995**, *374*, 594–595. [[CrossRef](#)]
7. Mason, S.F. Origins of biomolecular handedness. *Nature* **1984**, *311*, 19–23. [[CrossRef](#)]
8. Collins, A.N.; Sheldrake, G.; Crosby, J. *Chirality in Industry ii: Developments in the Commercial Manufacture and Applications of Optically Active Compounds*; John Wiley & Sons: Hoboken, NJ, USA, 1997; Volume 2.
9. Eliel, E.L.; Wilen, S.H. *Stereochemistry of Organic Compounds*; John Wiley & Sons: Hoboken, NJ, USA, 2008.
10. Hegstrom, R.A.; Kondepudi, D.K. The handedness of the universe. *Sci. Am.* **1990**, *262*, 108–115. [[CrossRef](#)]

11. Liu, M.; Zhang, L.; Wang, T. Supramolecular chirality in self-assembled systems. *Chem. Rev.* **2015**, *115*, 7304–7397. [[CrossRef](#)]
12. Duan, P.; Cao, H.; Zhang, L.; Liu, M. Gelation induced supramolecular chirality: Chirality transfer, amplification and application. *Soft Matter* **2014**, *10*, 5428–5448. [[CrossRef](#)]
13. Yamaguchi, T.; Kimura, T.; Matsuda, H.; Aida, T. Macroscopic spinning chirality memorized in spin-coated films of spatially designed dendritic zinc porphyrin j-aggregates. *Angew. Chem. Int. Ed.* **2004**, *43*, 6350–6355. [[CrossRef](#)] [[PubMed](#)]
14. Ribo, J.M.; Crusats, J.; Sagues, F.; Claret, J.; Rubires, R. Chiral sign induction by vortices during the formation of mesophases in stirred solutions. *Science* **2001**, *292*, 2063–2066. [[CrossRef](#)] [[PubMed](#)]
15. Azeroual, S.; Surprenant, J.; Lazzara, T.D.; Kocun, M.; Tao, Y.; Cuccia, L.A.; Lehn, J.-M. Mirror symmetry breaking and chiral amplification in foldamer-based supramolecular helical aggregates. *Chem. Commun.* **2012**, *48*, 2292–2294. [[CrossRef](#)] [[PubMed](#)]
16. DeRossi, U.; Dahne, S.; Meskers, S.C.J.; Dekkers, H. Spontaneous formation of chirality in j-aggregates showing davydov splitting. *Angew. Chem. Int. Ed.* **1996**, *35*, 760–763. [[CrossRef](#)]
17. Zhang, S.; Yang, S.; Lan, J.; Yang, S.; You, J. Helical nonracemic tubular coordination polymer gelators from simple achiral molecules. *Chem. Commun.* **2008**, 6170–6172. [[CrossRef](#)] [[PubMed](#)]
18. Saito, Y.; Hyuga, H. Colloquium: Homochirality: Symmetry breaking in systems driven far from equilibrium. *Rev. Mod. Phys.* **2013**, *85*, 603–621. [[CrossRef](#)]
19. Bonner, W.A. The origin and amplification of biomolecular chirality. *Orig. Life Evol. Biosph.* **1991**, *21*, 59–111. [[CrossRef](#)]
20. Luisi, P.L. *The Emergence of Life: From Chemical Origins to Synthetic Biology*; Cambridge University Press: Cambridge, UK, 2016.
21. Barron, L.D. Symmetry and molecular chirality. *Chem. Soc. Rev.* **1986**, *15*, 189–223. [[CrossRef](#)]
22. Cintas, P.; Viedma, C. On the physical basis of asymmetry and homochirality. *Chirality* **2012**, *24*, 894–908. [[CrossRef](#)]
23. Karunakaran, S.C.; Cafferty, B.J.; Weigert-Munoz, A.; Schuster, G.B.; Hud, N.V. Spontaneous symmetry breaking in the formation of supramolecular polymers: Implications for the origin of biological homochirality. *Angew. Chem. Int. Ed.* **2019**, *58*, 1453–1457. [[CrossRef](#)]
24. Alexander, A.J. Crystallization of sodium chlorate with d-glucose co-solute is not enantioselective. *Cryst. Growth Des.* **2008**, *8*, 2630–2632. [[CrossRef](#)]
25. Kondepudi, D.K.; Kaufman, R.J.; Singh, N. Chiral symmetry-breaking in sodium-chlorate crystallization. *Science* **1990**, *250*, 975–976. [[CrossRef](#)] [[PubMed](#)]
26. Kipping, F.S.; Pope, W.J. Lxiii.—Enantiomorphism. *J. Am. Chem. Soc.* **1898**, *73*, 606–617. [[CrossRef](#)]
27. Yuan, J.; Liu, M. Chiral molecular assemblies from a novel achiral amphiphilic 2-(heptadecyl) naphtha[2,3]imidazole through interfacial coordination. *J. Am. Chem. Soc.* **2003**, *125*, 5051–5056. [[CrossRef](#)] [[PubMed](#)]
28. Huang, X.; Li, C.; Jiang, S.; Wang, X.; Zhang, B.; Liu, M. Self-assembled spiral nanoarchitecture and supramolecular chirality in langmuir–blodgett films of an achiral amphiphilic barbituric acid. *J. Am. Chem. Soc.* **2004**, *126*, 1322–1323. [[CrossRef](#)] [[PubMed](#)]
29. Guo, P.; Zhang, L.; Liu, M. A supramolecular chiroptical switch exclusively from an achiral amphiphile. *Adv. Mater.* **2006**, *18*, 177–180. [[CrossRef](#)]
30. Elemans, J.A.A.W.; De Cat, I.; Xu, H.; De Feyter, S. Two-dimensional chirality at liquid-solid interfaces. *Chem. Soc. Rev.* **2009**, *38*, 722–736. [[CrossRef](#)] [[PubMed](#)]
31. Ernst, K. Amplification of chirality in two-dimensional molecular lattices. *Curr. Opin. Colloid Interface Sci.* **2008**, *13*, 54–59. [[CrossRef](#)]
32. Foster, J.S.; Frommer, J.E. Imaging of liquid-crystals using a tunnelling microscope. *Nature* **1988**, *333*, 542–545. [[CrossRef](#)]
33. Hough, L.E.; Spannuth, M.; Nakata, M.; Coleman, D.A.; Jones, C.D.; Dantlgraber, G.; Tschierske, C.; Watanabe, J.; Koerblova, E.; Walba, D.M.; et al. Chiral isotropic liquids from achiral molecules. *Science* **2009**, *325*, 452–456. [[CrossRef](#)]
34. Dressel, C.; Liu, F.; Prehm, M.; Zeng, X.; Ungar, G.; Tschierske, C. Dynamic mirror-symmetry breaking in bicontinuous cubic phases. *Angew. Chem. Int. Ed.* **2014**, *53*, 13115–13120. [[CrossRef](#)] [[PubMed](#)]

35. Tschierske, C.; Ungar, G. Mirror symmetry breaking by chirality synchronisation in liquids and liquid crystals of achiral molecules. *Chemphyschem* **2016**, *17*, 9–26. [[CrossRef](#)] [[PubMed](#)]
36. Keith, C.; Reddy, R.A.; Hauser, A.; Baumeister, U.; Tschierske, C. Silicon-containing polyphilic bent-core molecules: The importance of nanosegregation for the development of chirality and polar order in liquid crystalline phases formed by achiral molecules. *J. Am. Chem. Soc.* **2006**, *128*, 3051–3066. [[CrossRef](#)] [[PubMed](#)]
37. Young, W.R.; Aviram, A.; Cox, R.J. Stilbene derivatives—New class of room-temperature nematic liquids. *J. Am. Chem. Soc.* **1972**, *94*, 3976–3981. [[CrossRef](#)]
38. Qiu, Y.; Chen, P.; Liu, M. Evolution of various porphyrin nanostructures via an oil/aqueous medium: Controlled self-assembly, further organization, and supramolecular chirality. *J. Am. Chem. Soc.* **2010**, *132*, 9644–9652. [[CrossRef](#)] [[PubMed](#)]
39. Okano, K.; Taguchi, M.; Fujiki, M.; Yamashita, T. Circularly polarized luminescence of rhodamine b in a supramolecular chiral medium formed by a vortex flow. *Angew. Chem. Int. Ed.* **2011**, *50*, 12474–12477. [[CrossRef](#)] [[PubMed](#)]
40. Li, Y.; Wong, K.M.-C.; Wong, H.-L.; Yam, V.W.-W. Helical self-assembly and photopolymerization properties of achiral amphiphilic platinum(ii) diacetylene complexes of tridentate 2,6bis(1-alkylpyrazol-3-yl)pyridines. *ACS Appl. Mater. Inter.* **2016**, *8*, 17445–17453. [[CrossRef](#)]
41. Song, B.; Liu, B.; Jin, Y.; He, X.; Tang, D.; Wu, G.; Yin, S. Controlled self-assembly of helical nano-ribbons formed by achiral amphiphiles. *Nanoscale* **2015**, *7*, 930–935. [[CrossRef](#)]
42. Stals, P.J.M.; Korevaar, P.A.; Gillissen, M.A.J.; de Greef, T.F.A.; Fitie, C.F.C.; Sijbesma, R.P.; Palmans, A.R.A.; Meijer, E.W. Symmetry breaking in the self-assembly of partially fluorinated benzene-1,3,5-tricarboxamides. *Angew. Chem. Int. Ed.* **2012**, *51*, 11297–11301. [[CrossRef](#)]
43. Shen, Z.; Wang, T.; Liu, M. Macroscopic chirality of supramolecular gels formed from achiral tris(ethyl cinnamate) benzene-1,3,5-tricarboxamides. *Angew. Chem. Int. Ed.* **2014**, *53*, 13424–13428. [[CrossRef](#)]
44. Shen, Z.; Jiang, Y.; Wang, T.; Liu, M. Symmetry breaking in the supramolecular gels of an achiral gelator exclusively driven by pi-pi stacking. *J. Am. Chem. Soc.* **2015**, *137*, 16109–16115. [[CrossRef](#)] [[PubMed](#)]
45. Maity, A.; Gangopadhyay, M.; Basu, A.; Aute, S.; Babu, S.S.; Das, A. Counter anion driven homochiral assembly of a cationic achiral c3-symmetric gelator through ion-pair assisted hydrogen bond. *J. Am. Chem. Soc.* **2016**, *138*, 11113–11116. [[CrossRef](#)] [[PubMed](#)]
46. Sang, Y.; Duan, P.; Liu, M. Nanotrumpets and circularly polarized luminescent nanotwists hierarchically self-assembled from an achiral c3-symmetric ester. *Chem. Commun.* **2018**, *54*, 4025–4028. [[CrossRef](#)] [[PubMed](#)]
47. Kimura, M.; Hatanaka, T.; Nomoto, H.; Takizawa, J.; Fukawa, T.; Tatewaki, Y.; Shirai, H. Self-assembled helical nanofibers made of achiral molecular disks having molecular adapter. *Chem. Mater.* **2010**, *22*, 5732–5738. [[CrossRef](#)]
48. Pasteur, M.L. Recherches sur les relations qui peuvent exister entre la forme cristalline: La composition chimique et les sens de la polarisation rotatoire. *Ann. Chim. Phys.* **1848**, 442–459.
49. Pagni, R.M.; Compton, R.N. Asymmetric synthesis of optically active sodium chlorate and bromate crystals. *Cryst. Growth Des.* **2002**, *2*, 249–253. [[CrossRef](#)]
50. Kipping, F.S.; Pope, W.J. Stereochemistry and vitalism. *Nature* **1898**, *59*, 53. [[CrossRef](#)]
51. Koby, L.; Ningappa, J.B.; Dakessian, M.; Cuccia, L.A. Chiral crystallization of ethylenediamine sulfate. *J. Chem. Educ.* **2005**, *82*, 1043–1045.
52. Saito, Y.; Hyuga, H. Chirality selection in crystallization. *J. Phys. Soc. Jpn.* **2005**, *74*, 535–537. [[CrossRef](#)]
53. Ziach, K.; Jurczak, J. Mirror symmetry breaking upon spontaneous crystallization from a dynamic combinatorial library of macrocyclic imines. *Chem. Commun.* **2015**, *51*, 4306–4309. [[CrossRef](#)]
54. Chen, S.-C.; Zhang, J.; Yu, R.-M.; Wu, X.-Y.; Xie, Y.-M.; Wang, F.; Lu, C.-Z. Spontaneous asymmetrical crystallization of a three-dimensional diamondoid framework material from achiral precursors. *Chem. Commun.* **2010**, *46*, 1449–1451. [[CrossRef](#)] [[PubMed](#)]
55. Shu, C.-Y.; Huang, F.-P.; Yu, Q.; Yao, P.-F.; Bian, H.-D.; Lan, R.-Q.; Wei, B.-L. Ph-dependent co(ii) assemblies from achiral 2-benzothiazolylthioacetic acid: Crystal structures, symmetry breaking, and magnetic properties. *J. Coord. Chem.* **2015**, *68*, 2107–2120. [[CrossRef](#)]
56. Mineo, P.; Villari, V.; Scamporrino, E.; Micali, N. Supramolecular chirality induced by a weak thermal force. *Soft Matter* **2014**, *10*, 44–47. [[CrossRef](#)] [[PubMed](#)]

57. Wang, Y.; Zhou, D.; Li, H.; Li, R.; Zhong, Y.; Sun, X.; Sun, X. Hydrogen-bonded supercoil self-assembly from achiral molecular components with light-driven supramolecular chirality. *J. Mater. Chem. C* **2014**, *2*, 6402–6409. [[CrossRef](#)]
58. Hu, Q.; Wang, Y.; Jia, J.; Wang, C.; Feng, L.; Dong, R.; Sun, X.; Hao, J. Photoresponsive chiral nanotubes of achiral amphiphilic azobenzene. *Soft Matter* **2012**, *8*, 11492–11498. [[CrossRef](#)]
59. Romeo, A.; Castriciano, M.A.; Occhiuto, I.; Zagami, R.; Pasternack, R.F.; Scolaro, L.M. Kinetic control of chirality in porphyrin j-aggregates. *J. Am. Chem. Soc.* **2014**, *136*, 40–43. [[CrossRef](#)] [[PubMed](#)]
60. Katsonis, N.; Lacaze, E.; Feringa, B.L. Molecular chirality at fluid/solid interfaces: Expression of asymmetry in self-organised monolayers. *J. Mater. Chem. C* **2008**, *18*, 2065–2073. [[CrossRef](#)]
61. Perez-Garcia, L.; Amabilino, D.B. Spontaneous resolution, whence and whither: From enantiomorphic solids to chiral liquid crystals, monolayers and macro-and supra-molecular polymers and assemblies. *Chem. Soc. Rev.* **2007**, *36*, 941–967. [[CrossRef](#)]
62. Parschau, M.; Ernst, K.-H. Disappearing enantiomorphs: Single handedness in racemate crystals. *Angew. Chem. Int. Ed.* **2015**, *54*, 14422–14426. [[CrossRef](#)]
63. Sakaguchi, H.; Song, S.; Kojima, T.; Nakae, T. Homochiral polymerization-driven selective growth of graphene nanoribbons. *Nat. Chem.* **2017**, *9*, 57–63. [[CrossRef](#)]
64. George, L.; Gaines, J. *Insoluble Monolayers at Liquid-Gas Interfaces*; Interscience Publishers: New York, NY, USA, 1966.
65. Ulman, A. *An Introduction to Ultrathin Organic Films: From Langmuir-Blodgett to Self-Assembly*; Academic Press: Cambridge, MA, USA, 2013.
66. Tahara, K.; Yamaga, H.; Ghijsens, E.; Inukai, K.; Adisojoso, J.; Blunt, M.O.; De Feyter, S.; Tobe, Y. Control and induction of surface-confined homochiral porous molecular networks. *Nat. Chem.* **2011**, *3*, 714–719. [[CrossRef](#)]
67. Sang, Y.; Yang, D.; Duan, P.; Liu, M. Towards homochiral supramolecular entities from achiral molecules by vortex mixing-accompanied self-assembly. *Chem. Sci.* **2019**, *10*, 2718–2724. [[CrossRef](#)] [[PubMed](#)]
68. Barth, J.V. Molecular architectonic on metal surfaces. *Annu. Rev. Phys. Chem.* **2007**, *58*, 375–407. [[CrossRef](#)] [[PubMed](#)]
69. Bartels, L. Tailoring molecular layers at metal surfaces. *Nat. Chem.* **2010**, *2*, 87–95. [[CrossRef](#)]
70. Link, D.R.; Natale, G.; Shao, R.; Maclennan, J.E.; Clark, N.A.; Korblova, E.; Walba, D.M. Spontaneous formation of macroscopic chiral domains in a fluid smectic phase of achiral molecules. *Science* **1997**, *278*, 1924–1927. [[CrossRef](#)] [[PubMed](#)]
71. Tschierske, C. Development of structural complexity by liquid-crystal self-assembly. *Angew. Chem. Int. Ed.* **2013**, *52*, 8828–8878. [[CrossRef](#)]
72. Stoddart, J.F. Thither supramolecular chemistry? *Nat. Chem.* **2009**, *1*, 14–15. [[CrossRef](#)]
73. Tschierske, C. Liquid crystals materials design and self-assembly preface. In *Liquid Crystals: Materials Design and Self-Assembly*; Tschierske, C., Ed.; Springer Science & Business Media: Berlin, Germany, 2012; Volume 318, pp. IX–X.
74. Goodby, J.W. The nanoscale engineering of nematic liquid crystals for displays. *Liq. Cryst.* **2011**, *38*, 1363–1387. [[CrossRef](#)]
75. Cantekin, S.; de Greef, T.F.; Palmans, A.R. Benzene-1, 3, 5-tricarboxamide: A versatile ordering moiety for supramolecular chemistry. *Chem. Soc. Rev.* **2012**, *41*, 6125–6137. [[CrossRef](#)]
76. Desiraju, G.R.; Steiner, T. *The Weak Hydrogen Bond: In Structural Chemistry and Biology*; International Union of Crystal: Weinheim, Germany, 2001; Volume 9.
77. Kimizuka, N.; Kawasaki, T.; Hirata, K.; Kunitake, T. Tube-like nanostructures composed of networks of complementary hydrogen bonds. *J. Am. Chem. Soc.* **1995**, *117*, 6360–6361. [[CrossRef](#)]
78. George, S.J.; Tomović, Ž.; Smulders, M.M.; de Greef, T.F.; Leclère, P.E.; Meijer, E.W.; Schenning, A.P. Helicity induction and amplification in an oligo (p-phenylenevinylene) assembly through hydrogen-bonded chiral acids. *Angew. Chem. Int. Ed.* **2007**, *46*, 8206–8211. [[CrossRef](#)] [[PubMed](#)]
79. Yan, X.; Li, S.; Pollock, J.B.; Cook, T.R.; Chen, J.; Zhang, Y.; Ji, X.; Yu, Y.; Huang, F.; Stang, P.J. Supramolecular polymers with tunable topologies via hierarchical coordination-driven self-assembly and hydrogen bonding interfaces. *Proc. Natl. Acad. Sci. USA* **2013**, *110*, 15585–15590. [[CrossRef](#)] [[PubMed](#)]

80. Ji, X.; Shi, B.; Wang, H.; Xia, D.; Jie, K.; Wu, Z.L.; Huang, F. Supramolecular construction of multifluorescent gels: Interfacial assembly of discrete fluorescent gels through multiple hydrogen bonding. *Adv. Mater.* **2015**, *27*, 8062–8066. [[CrossRef](#)] [[PubMed](#)]
81. Buchs, J.; Vogel, L.; Janietz, D.; Prehm, M.; Tschierske, C. Chirality synchronization of hydrogen-bonded complexes of achiral n-heterocycles. *Angew. Chem. Int. Ed.* **2017**, *56*, 280–284. [[CrossRef](#)] [[PubMed](#)]
82. Ding, S.; Gao, Y.; Ji, Y.; Wang, Y.; Liu, Z. Homochiral crystallization of single-stranded helical coordination polymers: Generated by the structure of auxiliary ligands or spontaneous symmetry breaking. *CrystEngComm* **2013**, *15*, 5598–5601. [[CrossRef](#)]
83. Wu, S.T.; Wu, Y.R.; Kang, Q.Q.; Zhang, H.; Long, L.S.; Zheng, Z.; Huang, R.B.; Zheng, L.S. Chiral symmetry breaking by chemically manipulating statistical fluctuation in crystallization. *Angew. Chem. Int. Ed.* **2007**, *46*, 8475–8479. [[CrossRef](#)] [[PubMed](#)]
84. Meng, W.; Ronson, T.K.; Nitschke, J.R. Symmetry breaking in self-assembled m4l6 cage complexes. *Proc. Natl. Acad. Sci. USA* **2013**, *110*, 10531–10535. [[CrossRef](#)]
85. Zhou, T.-H.; Zhang, J.; Zhang, H.-X.; Feng, R.; Mao, J.-G. A ligand-conformation driving chiral generation and symmetry-breaking crystallization of a zinc (ii) organoarsenate. *Chem. Commun.* **2011**, *47*, 8862–8864. [[CrossRef](#)] [[PubMed](#)]
86. Mamula, O.; von Zelewsky, A. Supramolecular coordination compounds with chiral pyridine and polypyridine ligands derived from terpenes. *Coord. Chem. Rev.* **2003**, *242*, 87–95. [[CrossRef](#)]
87. Zhang, L.; Qin, L.; Wang, X.; Cao, H.; Liu, M. Supramolecular chirality in self-assembled soft materials: Regulation of chiral nanostructures and chiral functions. *Adv. Mater.* **2014**, *26*, 6959–6964. [[CrossRef](#)] [[PubMed](#)]
88. Pérez-García, L.; Amabilino, D.B. Spontaneous resolution under supramolecular control. *Chem. Soc. Rev.* **2002**, *31*, 342–356. [[CrossRef](#)] [[PubMed](#)]
89. Janssen, P.G.A.; Ruiz-Carretero, A.; Gonzalez-Rodriguez, D.; Meijer, E.W.; Schenning, A.P. Ph-switchable helicity of DNA-templated assemblies. *Angew. Chem. Int. Ed.* **2009**, *48*, 8103–8106. [[CrossRef](#)] [[PubMed](#)]
90. Kondepudi, D.K.; Nelson, G.W. Weak neutral currents and the origin of biomolecular chirality. *Nature* **1985**, *314*, 438–441. [[CrossRef](#)]
91. Berger, R.; Quack, M. Electroweak quantum chemistry of alanine: Parity violation in gas and condensed phases. *Chemphyschem* **2000**, *1*, 57–60. [[CrossRef](#)]
92. Sorrenti, A.; Rodriguez-Trujillo, R.; Amabilino, D.B.; Puigmarti-Luis, J. Milliseconds make the difference in the far-from-equilibrium self-assembly of supramolecular chiral nanostructures. *J. Am. Chem. Soc.* **2016**, *138*, 6920–6923. [[CrossRef](#)]
93. Sun, J.; Li, Y.; Yan, F.; Liu, C.; Sang, Y.; Tian, F.; Feng, Q.; Duan, P.; Zhang, L.; Shi, X.; et al. Control over the emerging chirality in supramolecular gels and solutions by chiral microvortices in milliseconds. *Nat. Commun.* **2018**, *9*, 2599. [[CrossRef](#)] [[PubMed](#)]
94. Kuhn, A.; Fischer, P. Absolute asymmetric reduction based on the relative orientation of achiral reactants. *Angew. Chem. Int. Ed.* **2009**, *48*, 6857–6860. [[CrossRef](#)]
95. Kawasaki, T.; Kamimura, S.; Amihara, A.; Suzuki, K.; Soai, K. Enantioselective C–C bond formation as a result of the oriented prochirality of an achiral aldehyde at the single-crystal face upon treatment with a dialkyl zinc vapor. *Angew. Chem. Int. Ed.* **2011**, *50*, 6796–6798. [[CrossRef](#)]
96. Fang, Y.; Ghijsens, E.; Ivasenko, O.; Cao, H.; Noguchi, A.; Mali, K.S.; Tahara, K.; Tobe, Y.; De Feyter, S. Dynamic control over supramolecular handedness by selecting chiral induction pathways at the solution-solid interface. *Nat. Chem.* **2016**, *8*, 711–717. [[CrossRef](#)]
97. Wilson, A.J.; Masuda, M.; Sijbesma, R.P.; Meijer, E.W. Chiral amplification in the transcription of supramolecular helicity into a polymer backbone. *Angew. Chem. Int. Ed.* **2005**, *44*, 2275–2279. [[CrossRef](#)]
98. Palmans, A.R.; Meijer, E.E.W. Amplification of chirality in dynamic supramolecular aggregates. *Angew. Chem. Int. Ed.* **2007**, *46*, 8948–8968. [[CrossRef](#)] [[PubMed](#)]
99. Smulders, M.M.J.; Schenning, A.P.H.J.; Meijer, E.W. Insight into the mechanisms of cooperative self-assembly: The “sergeants-and-soldiers” principle of chiral and achiral C<sub>3</sub>-symmetrical discotic triamides. *J. Am. Chem. Soc.* **2008**, *130*, 606–611. [[CrossRef](#)] [[PubMed](#)]
100. Flores, J.J.; Bonner, W.A.; Massey, G.A. Asymmetric photolysis of (rs)-leucine with circularly polarized uv light. *J. Am. Chem. Soc.* **1977**, *99*, 3622–3625. [[CrossRef](#)] [[PubMed](#)]

101. Bailey, J.; Chrysostomou, A.; Hough, J.H.; Gledhill, T.M.; McCall, A.; Clark, S.; Menard, F.; Tamura, M. Circular polarization in star-formation regions: Implications for biomolecular homochirality. *Science* **1998**, *281*, 672–674. [[CrossRef](#)] [[PubMed](#)]
102. Kim, J.; Lee, J.; Kim, W.Y.; Kim, H.; Lee, S.; Lee, H.C.; Lee, Y.S.; Seo, M.; Kim, S.Y. Induction and control of supramolecular chirality by light in self-assembled helical nanostructures. *Nat. Commun.* **2015**, *6*, 6959. [[CrossRef](#)] [[PubMed](#)]
103. Micali, N.; Engelkamp, H.; van Rhee, P.G.; Christianen, P.C.M.; Scolaro, L.M.; Maan, J.C. Selection of supramolecular chirality by application of rotational and magnetic forces. *Nat. Chem.* **2012**, *4*, 201–207. [[CrossRef](#)] [[PubMed](#)]
104. D'Urso, A.; Randazzo, R.; Lo Faro, L.; Purrello, R. Vortexes and nanoscale chirality. *Angew. Chem. Int. Ed.* **2010**, *49*, 108–112. [[CrossRef](#)] [[PubMed](#)]
105. Escudero, C.; Crusats, J.; Díez-Pérez, I.; El-Hachemi, Z.; Ribó, J.M. Folding and hydrodynamic forces in j-aggregates of 5-phenyl-10, 15, 20-tris (4-sulfophenyl) porphyrin. *Angew. Chem. Int. Ed.* **2006**, *118*, 8200–8203. [[CrossRef](#)]
106. Ribo, J.M.; El-Hachemi, Z.; Arteaga, O.; Canillas, A.; Crusats, J. Hydrodynamic effects in soft-matter self-assembly: The case of j-aggregates of amphiphilic porphyrins. *Chem. Rec.* **2017**, *17*, 713–724. [[CrossRef](#)] [[PubMed](#)]
107. Crusats, J.; El-Hachemi, Z.; Ribo, J.M. Hydrodynamic effects on chiral induction. *Chem. Soc. Rev.* **2010**, *39*, 569–577. [[CrossRef](#)]
108. Aquilanti, V.; Maciel, G.S. Observed molecular alignment in gaseous streams and possible chiral effects in vortices and in surface scattering. *Orig. Life Evol. Biosph.* **2006**, *36*, 435–441. [[CrossRef](#)] [[PubMed](#)]
109. Jalilah, A.J.; Asanoma, F.; Fujiki, M. Unveiling controlled breaking of the mirror symmetry of eu(fod)(3) with alpha-/beta-pinene and binap by circularly polarised luminescence (cpl), cpl excitation, and f-19-/p-31{h-1}-nmr spectra and mulliken charges. *Inorg. Chem. Front.* **2018**, *5*, 2718–2733. [[CrossRef](#)]
110. Fujiki, M. Supramolecular chirality: Solvent chirality transfer in molecular chemistry and polymer chemistry. *Symmetry-Basel* **2014**, *6*, 677–703. [[CrossRef](#)]
111. McBride, J.M.; Carter, R.L. Spontaneous resolution by stirred crystallization. *Angew. Chem. Int. Ed.* **1991**, *30*, 293–295. [[CrossRef](#)]
112. Kondepudi, D.K.; Bullock, K.L.; Digits, J.A.; Yarborough, P.D. Stirring rate as a critical parameter in chiral-symmetry breaking crystallization. *J. Am. Chem. Soc.* **1995**, *117*, 401–404. [[CrossRef](#)]
113. Viedma, C. Chiral symmetry breaking during crystallization: Complete chiral purity induced by nonlinear autocatalysis and recycling. *Phys. Rev. Lett.* **2005**, *94*, 065504. [[CrossRef](#)] [[PubMed](#)]
114. Sogutoglu, L.C.; Steendam, R.R.; Meekes, H.; Vlieg, E.; Rutjes, F.P. Viedma ripening: A reliable crystallisation method to reach single chirality. *Chem. Soc. Rev.* **2015**, *44*, 6723–6732. [[CrossRef](#)] [[PubMed](#)]
115. Palmans, A.R.A. Deracemisations under kinetic and thermodynamic control. *Mol. Syst. Des. Eng.* **2017**, *2*, 34–46. [[CrossRef](#)]
116. Steendam, R.R.; Verkade, J.M.; van Benthem, T.J.; Meekes, H.; van Enckevort, W.J.; Raap, J.; Rutjes, F.P.; Vlieg, E. Emergence of single-molecular chirality from achiral reactants. *Nat. Commun.* **2014**, *5*, 5543. [[CrossRef](#)] [[PubMed](#)]
117. Engwerda, A.H.J.; Koning, N.; Tinnemans, P.; Meekes, H.; Bickelhaupt, F.M.; Rutjes, F.P.J.T.; Vlieg, E. Deracemization of a racemic allylic sulfoxide using viedma ripening. *Cryst. Growth Des.* **2017**, *17*, 4454–4457. [[CrossRef](#)] [[PubMed](#)]
118. Noorduyn, W.L.; Meekes, H.; van Enckevort, W.J.P.; Millemaggi, A.; Leeman, M.; Kaptein, B.; Kellogg, R.M.; Vlieg, E. Complete deracemization by attrition-enhanced ostwald ripening elucidated. *Angew. Chem. Int. Ed.* **2008**, *47*, 6445–6447. [[CrossRef](#)] [[PubMed](#)]
119. Hein, J.E.; Cao, B.H.; Viedma, C.; Kellogg, R.M.; Blackmond, D.G. Pasteur's tweezers revisited: On the mechanism of attrition-enhanced deracemization and resolution of chiral conglomerate solids. *J. Am. Chem. Soc.* **2012**, *134*, 12629–12636. [[CrossRef](#)] [[PubMed](#)]
120. Noorduyn, W.L.; Izumi, T.; Millemaggi, A.; Leeman, M.; Meekes, H.; Van Enckevort, W.J.P.; Kellogg, R.M.; Kaptein, B.; Vlieg, E.; Blackmond, D.G. Emergence of a single solid chiral state from a nearly racemic amino acid derivative. *J. Am. Chem. Soc.* **2008**, *130*, 1158–1159. [[CrossRef](#)] [[PubMed](#)]
121. Viedma, C.; Ortiz, J.E.; de Torres, T.; Izumi, T.; Blackmond, D.G. Evolution of solid phase homochirality for a proteinogenic amino acid. *J. Am. Chem. Soc.* **2008**, *130*, 15274–15275. [[CrossRef](#)] [[PubMed](#)]

122. Tsogoeva, S.B.; Wei, S.; Freund, M.; Mauksch, M. Generation of highly enantioenriched crystalline products in reversible asymmetric reactions with racemic or achiral catalysts. *Angew. Chem. Int. Ed.* **2009**, *48*, 590–594. [[CrossRef](#)] [[PubMed](#)]
123. Viedma, C.; Cintas, P. Homochirality beyond grinding: Deracemizing chiral crystals by temperature gradient under boiling. *Chem. Commun.* **2011**, *47*, 12786–12788. [[CrossRef](#)] [[PubMed](#)]
124. Suwannasang, K.; Flood, A.E.; Rougeot, C.; Coquerel, G. Use of programmed damped temperature cycles for the deracemization of a racemic suspension of a conglomerate forming system. *Org. Process Res. Dev.* **2017**, *21*, 623–630. [[CrossRef](#)]
125. Ribó, J.M.; Hochberg, D.; Crusats, J.; El-Hachemi, Z.; Moyano, A. Spontaneous mirror symmetry breaking and origin of biological homochirality. *J. R. Soc. Interface* **2017**, *14*, 20170699. [[CrossRef](#)]
126. Rubires, R.; Farrera, J.A.; Ribo, J.M. Stirring effects on the spontaneous formation of chirality in the homoassociation of diprotonated meso-tetraphenylsulfonato porphyrins. *Chem. Eur. J.* **2001**, *7*, 436–446. [[CrossRef](#)]
127. Raudino, A.; Pannuzzo, M. Hydrodynamic-induced enantiomeric enrichment of self-assemblies: Role of the solid-liquid interface in chiral nucleation and seeding. *J. Chem. Phys.* **2012**, *137*, 134902. [[CrossRef](#)]
128. Kitagawa, Y.; Segawa, H.; Ishii, K. Magneto-chiral dichroism of organic compounds. *Angew. Chem. Int. Ed.* **2011**, *50*, 9133–9136. [[CrossRef](#)] [[PubMed](#)]
129. Hamba, F.; Niimura, K.; Kitagawa, Y.; Ishii, K. Helicity transfer in rotary evaporator flow. *Phys. Fluids* **2014**, *26*, 017101. [[CrossRef](#)]
130. Heffern, M.C.; Matosziuk, L.M.; Meade, T.J. Lanthanide probes for bioresponsive imaging. *Chem. Rev.* **2014**, *114*, 4496–4539. [[CrossRef](#)] [[PubMed](#)]
131. Carr, R.; Evans, N.H.; Parker, D. Lanthanide complexes as chiral probes exploiting circularly polarized luminescence. *Chem. Soc. Rev.* **2012**, *41*, 7673–7686. [[CrossRef](#)] [[PubMed](#)]
132. Schadt, M. Liquid crystal materials and liquid crystal displays. *Annu. Rev. Mater. Sci.* **1997**, *27*, 305–379. [[CrossRef](#)]
133. Kim, D.-Y.; Kim, D.-Y. Potential application of spintronic light-emitting diode to binocular vision for three-dimensional display technology. *J. Korean Phys. Soc.* **2006**, *49*, 505–508.
134. Zinna, F.; Di Bari, L. Lanthanide circularly polarized luminescence: Bases and applications. *Chirality* **2015**, *27*, 1–13. [[CrossRef](#)]
135. Muller, G. Luminescent chiral lanthanide(iii) complexes as potential molecular probes. *Dalton Trans.* **2009**, 9692–9707. [[CrossRef](#)]
136. Wagenknecht, C.; Li, C.-M.; Reingruber, A.; Bao, X.-H.; Goebel, A.; Chen, Y.-A.; Zhang, Q.; Chen, K.; Pan, J.-W. Experimental demonstration of a heralded entanglement source. *Nat. Photonics* **2010**, *4*, 549–552. [[CrossRef](#)]
137. Xu, Y.; Yang, G.; Xia, H.; Zou, G.; Zhang, Q.; Gao, J. Enantioselective synthesis of helical polydiacetylene by application of linearly polarized light and magnetic field. *Nat. Commun.* **2014**, *5*, 5050. [[CrossRef](#)]
138. Tang, Y.; Cohen, A.E. Enhanced enantioselectivity in excitation of chiral molecules by superchiral light. *Science* **2011**, *332*, 333–336. [[CrossRef](#)] [[PubMed](#)]
139. Sato, I.; Sugie, R.; Matsueda, Y.; Furumura, Y.; Soai, K. Asymmetric synthesis utilizing circularly polarized light mediated by the photoequilibrium of chiral olefins in conjunction with asymmetric autocatalysis. *Angew. Chem. Int. Ed.* **2004**, *43*, 4490–4492. [[CrossRef](#)] [[PubMed](#)]
140. Kawasaki, T.; Sato, M.; Ishiguro, S.; Saito, T.; Morishita, Y.; Sato, I.; Nishino, H.; Inoue, Y.; Soai, K. Enantioselective synthesis of near enantiopure compound by asymmetric autocatalysis triggered by asymmetric photolysis with circularly polarized light. *J. Am. Chem. Soc.* **2005**, *127*, 3274–3275. [[CrossRef](#)] [[PubMed](#)]
141. Yang, Y.; da Costa, R.C.; Fuchter, M.J.; Campbell, A.J. Circularly polarized light detection by a chiral organic semiconductor transistor. *Nat. Photonics* **2013**, *7*, 634–638. [[CrossRef](#)]
142. Meinert, C.; Bredehoeft, J.H.; Filippi, J.-J.; Baraud, Y.; Nahon, L.; Wien, F.; Jones, N.C.; Hoffmann, S.V.; Meierhenrich, U.J. Anisotropy spectra of amino acids. *Angew. Chem. Int. Ed.* **2012**, *51*, 4484–4487. [[CrossRef](#)] [[PubMed](#)]
143. Meinert, C.; Hoffmann, S.V.; Cassam-Chenai, P.; Evans, A.C.; Giri, C.; Nahon, L.; Meierhenrich, U.J. Photonenergy-controlled symmetry breaking with circularly polarized light. *Angew. Chem. Int. Ed.* **2014**, *53*, 210–214. [[CrossRef](#)] [[PubMed](#)]

144. He, C.; Yang, G.; Kuai, Y.; Shan, S.; Yang, L.; Hu, J.; Zhang, D.; Zhang, Q.; Zou, G. Dissymmetry enhancement in enantioselective synthesis of helical polydiacetylene by application of superchiral light. *Nat. Commun.* **2018**, *9*, 5117. [[CrossRef](#)]
145. Fujiki, M.; Kawagoe, Y.; Nakano, Y.; Nakao, A. Mirror-symmetry-breaking in poly (9,9-di-n-octylfluorenyl-2,7-diyl)-alt-biphenyl (pf8p2) is susceptible to terpene chirality, achiral solvents, and mechanical stirring. *Molecules* **2013**, *18*, 7035–7057. [[CrossRef](#)]
146. Noorduin, W.L.; Bode, A.A.C.; van der Meijden, M.; Meekes, H.; van Etteger, A.F.; van Enckevort, W.J.P.; Christianen, P.C.M.; Kaptein, B.; Kellogg, R.M.; Rasing, T.; et al. Complete chiral symmetry breaking of an amino acid derivative directed by circularly polarized light. *Nat. Chem.* **2009**, *1*, 729–732. [[CrossRef](#)]
147. Japp, F.R. Asymmetry and vitalism. *Nature* **1898**, *58*, 616–618. [[CrossRef](#)]
148. Feringa, B.L.; Van Delden, R.A. Absolute asymmetric synthesis: The origin, control, and amplification of chirality. *Angew. Chem. Int. Ed.* **1999**, *38*, 3418–3438. [[CrossRef](#)]
149. Yamagata, Y. A hypothesis for the asymmetric appearance of biomolecules on earth. *J. Theor. Biol.* **1966**, *11*, 495. [[CrossRef](#)]
150. Avalos, M.N.; Babiano, R.; Cintas, P.; Jiménez, J.L.; Palacios, J.C. From parity to chirality: Chemical implications revisited. *Tetrahedron Asymmetry* **2000**, *11*, 2845–2874. [[CrossRef](#)]



© 2019 by the authors. Licensee MDPI, Basel, Switzerland. This article is an open access article distributed under the terms and conditions of the Creative Commons Attribution (CC BY) license (<http://creativecommons.org/licenses/by/4.0/>).